II International Conference on Particle-based Methods - Fundamentals and Applications
PARTICLES 2011
E. Oñate and D.R.J. Owen (Eds)

PERMEABILITY ASSESSMENT OF HETEROGENEOUS POROUS MEDIA USING THE LATTICE BOLTZMANN METHOD

B. Jones, Y. T. Feng

Civil and Computational Engineering Centre
College of Engineering, Swansea University
Swansea, SA2 8PP, UK
email: 403113@swan.ac.uk

Key words: Lattice Boltzmann, Material Characterisation, Permeability, Partial Bounce-back

Abstract. Material characterisation is one of the most important aspects of accurate numerical modelling; correct material properties must be obtained for the correct behaviour to be observed. Traditionally permeability is measured by applying a constant/falling head test to a material sample, where such tests may involve many samples at varying pressure gradients. However current X-Ray micro-tomography techniques allow us to avoid physical lab tests by providing the ability to reproduce a voxelised representation of the internal structure of a porous medium. The Lattice Boltzmann Method may then be used to model a pressure induced flow field within the sample so that permeability may be numerically approximated. Typically this process is carried out after a thresholding procedure has been applied to the voxelised geometry to split it into definite solid and void spaces, at the expense of accurate representation of the geometry. In an attempt to better represent the porous medium the Immersed Moving Boundary technique was applied in such a way that it partially applies the bounce back boundary condition so that the strength of this application scales with the porosity of a given lattice node. This allows us to consider directly raw voxel values, avoiding the need for any thresholding procedure. To validate this hypothesis two test cases were explored in 2D; flow past a periodic array of cylinders by use of a unit cell model, and flow through a simple heterogeneous porous medium. Results were compared with analytical expressions where available, and published expressions for permeability evaluation of porous media. Results were found to be in good agreement with the available expressions.

1 INTRODUCTION

Accurate assessment of material permeability is a challenge encountered by many industrial organizations, in particular those engaged in Oil and Gas production. When such an organization requires knowledge of material permeability, they must gather a set of samples of sufficient size and submit them to a laboratory where a constant head test may be applied to assess permeability. Such tests may be destructive and time consuming, adding cost to an operation. It would be easy to assume that gathering samples is cheap; however if one considers the fact that these organizations may typically require knowledge of the permeability of rock which exists kilometres below the earth's surface, then it may also be seen that gathering material samples is in itself an extremely costly venture. In order to gain access to rock material at such depth a borehole must be drilled, and drilling must then be interrupted as and when material samples are to be extracted. This procedure operates on the assumption that the cuttings produced during drilling are too small to be subjected to traditional laboratory scale testing. It is therefore desirable to develop alternative means of permeability evaluation which are able to consider drill cuttings, the gathering of which has no impact on the drilling schedule of a borehole.

The Lattice Boltzmann Method[1] (LBM) has become a popular method in the field of porous media flow modelling,[2,3] in large part due to the simplicity of constructing a lattice which may represent heterogeneous porous media. Since the LBM operates on a regular lattice, in most cases a square lattice, one can avoid the complexities of meshing routines required by more traditional methods such as the Finite Volume or Finite Element methods. The LBM was originally derived from the Boltzmann equation, which describes the statistical likelihood that a particle exists at any given point in space and time with a given momentum. In the LBM, space and momentum are discretized so that particles may exist only at specific points with momentum aligned to a given set of vectors. The method is computationally cheap and efficient and may be parallelized with ease. Interaction between a fluid and a solid within an LBM model can be easily accounted for by use of what is known as the *bounce back* boundary condition, an extremely simple boundary condition which serves only to reflect any momentum incoming to the boundary. Within an LBM model any particular computational node, or lattice node, may have the bounce back condition imposed upon it. The result of the bounce back boundary is an *almost* no-slip condition at the interface between a bounce back node and a fluid node. The bounce back boundary condition therefore provides the ability to simply represent what may be a complex geometry, though its use does bring a significant drawback in so far as curved and inclined boundaries can only be represented using a *staircase* approximation.

X-Ray Micro-tomography (micro-CT) provides the ability to determine the internal micro structure of rock samples, and the LBM represents a suitable method for modelling the flow of fluids through this micro structure. A micro-CT scan of a rock sample would return a voxelised representation of the rock micro-structure, previous studies in this field have applied a thresholding procedure[3] to the voxelised geometry so that the bounce back condition may be applied to represent the rock medium. The goal of this study is to explore a way to avoid this thresholding procedure by novel use of the Immersed Moving Boundary method for LBM[4] in order to directly consider the voxelised geometry produced by a micro-CT scan, so that material permeability may be numerically approximated.

The use of the LBM, and aforementioned boundary conditions, with respect to permeability analysis was explored with a series of 2D test cases. These test cases include flow past a periodic array of hexagonally packed cylinders, flow through a homogeneous porous medium and flow through a simple heterogeneous porous medium.

2 PERMEABILITY ASSESSMENT

This section details methods by which the permeability of a porous medium may be analysed, both physically and computationally. In both physical and computational testing Darcy's equation is employed:

$$q = \frac{-k}{\mu} \nabla P \tag{1}$$

which includes terms for flux, q, viscosity, μ, pressure gradient, ∇P and finally material permeability, k in which we are interested. Darcy's equation defines a linear relationship between the flux, q, and pressure gradient, ∇P.

2.1 Physical Testing

A typical technique employed to assess the permeability of a material sample is the constant head test. The constant head test exploits the relationship between fluid flux, an applied pressure gradient and material permeability, as defined by Darcy's equation (1). When carrying out a constant head test on a material sample, the sample is initially saturated with fluid, a pressure gradient is then applied across the sample and the resultant volumetric flow rate is measured. Since the fluid viscosity is known, a known pressure gradient is applied, and the volumetric flowrate can be measured, Darcy's equation may then be used to calculate the permeability of the material sample.

2.2 Computational Testing

Computational permeability analysis is carried out with an identical methodology to physical permeability analysis. If the internal micro structure of a porous medium is known, it may be reproduced in a computational domain; using current CFD technology, in this case the LBM, one can then impose a pressure driven flow upon a computational domain. The fluid flux through this domain may be approximated by inspection of the results of the modelled pressure driven flow and, as long as the model parameters define a case where the modelled fluid is of known viscosity, the permeability of the modelled sample may be approximated.

3 NUMERICAL TECHNIQUE

The numerical techniques employed in this study are detailed and explained within this section, including the standard Lattice Boltzmann formulation, the simple bounce back no slip condition, and an Immersed Moving Boundary technique.[4] A brief description of

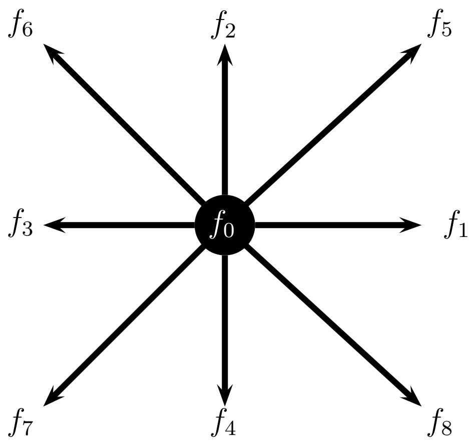

Figure 1: The Lattice Site

the Zhou/He boundary condition[5] is also included as it is used in this study to impose a pressure gradient upon the considered computational domains.

3.1 The Lattice Boltzmann Method

The standard DdQq Lattice Boltzmann scheme with an LBGK collision term[6] operates on a d-dimensional square lattice of lattice nodes connected by $q-1$ vectors. Since this study is concerned with 2D test cases only the D2Q9 lattice node was used, a diagram of which shown in Fig. 1. The D2Q9 lattice, and indeed any compatible lattice, consists of evenly spaced lattice nodes separated by a distance, h, in every dimension. Each lattice node is connected to its neighbours by 8 vectors, $\mathbf{e}_i$, and each vector has a particle distribution function (PDF), $\mathbf{f}_i$, associated with it along with a ninth "rest" PDF. If the numbering convention applied to the lattice node shown in Fig. 1 is respected, the corresponding vectors, $\mathbf{e}_i$, are given by:

$$\begin{aligned} \mathbf{e}_0 &= (0,0) \\ \mathbf{e}_i &= C\left(\cos\frac{\pi(i-1)}{2}, \sin\frac{\pi(i-1)}{2}\right)(i=1,...,4) \\ \mathbf{e}_i &= C\left(\cos\frac{\pi(2i-9)}{4}, \sin\frac{\pi(2i-9)}{4}\right)(i=5,...,8) \end{aligned} \tag{2}$$

in which the lattice speed, C, is related to the distance between the lattice nodes, h, and the discrete lattice time step, Δt,

$$C = h/\Delta t \tag{3}$$

The evolution of these PDF's is defined by the LBGK Lattice Boltzmann equation:

$$f_i(\mathbf{x} + \mathbf{e}_i \Delta t, t + \Delta t) - f_i(\mathbf{x}, t) = \frac{1}{\tau}(f_i^{eq}(\rho, \mathbf{u}) - f_i(\mathbf{x}, t)) \tag{4}$$

where the additional terms, ρ, $\mathbf{x}$ and τ are respectively the fluid density, position and relaxation time of a given lattice node. The relaxation time is a non-dimensional control parameter of a Lattice Boltzmann model, and defines the strength of the LBGK collision process which represents a relaxation to some equilibrium state. In terms of the LBM, the equilibrium state is defined by the equilibrium particle distribution function,

$$f_i^{eq} = \omega_i \rho \left(1 + \frac{3}{C^2}\mathbf{e}_i \cdot \mathbf{v} + \frac{9}{2C^4}(\mathbf{e}_i \cdot \mathbf{v})^2 - \frac{3}{2C^2}\mathbf{v} \cdot \mathbf{v}\right) \tag{5}$$

in which the weighting factors, ω_i, are:

$$\omega_0 = \frac{4}{9}, \quad \omega_{1,2,3,4} = \frac{1}{9}, \quad \omega_{5,5,6,8} = \frac{1}{36} \tag{6}$$

The macroscopic values of density, ρ, and momentum, $\rho\mathbf{u}$, can be calculated for each lattice node by,

$$\rho = \sum_i f_i \tag{7}$$

$$\rho\mathbf{u} = \sum_i \mathbf{e}_i f_i \tag{8}$$

respectivly. The pressure, P, is related to the density, ρ, as:

$$P = C_s^2 \rho \tag{9}$$

where the lattice speed of sound, C_s, is:

$$C_s = C/\sqrt{3} \tag{10}$$

Also, the fluid viscosity is related to the parameters in LBM as:

$$\nu = \frac{1}{3}(\tau - \frac{1}{2})\frac{h^2}{\Delta t} \tag{11}$$

Equation (4) dictates an evolution procedure for the PDF's that can be split into two stages; streaming, represented by the left hand side of the equation; and collision, represented by the right hand side of the equation. The collision step in this formulation is an LBGK collision process which, as stated, represents a relaxation towards an equilibrium state. The streaming step serves only to propagate PDF's from the lattice node in question, to its nearest neighbours. As can be seen, any numerical computation occurs only in the collision stage; furthermore for any given lattice node operating under the standard LBM scheme all computations are purely local. In terms of computational implementation the streaming step is in its simplest form a memory transfer operation, where PDF's are passed from one location in memory to another. Based on this it should be clear that the LBM for single phase fluid flows lends itself very well to parallel processing.

3.2 No Slip - Bounce Back

The No-Slip boundary condition is fundamental to fluid mechanics, and it implies that fluid in contact with a solid surface will travel at a velocity equal to the velocity of the surface. Due to the nature of the LBM, imposing a fixed velocity, or density, at a point in space is non-trivial. Equation (8) relates the effective momentum at a lattice node to its PDF's, so to fix the velocity at any given lattice node the relationship defined by this equation must be preserved. Unfortunately since equation (8) is the only equation available relating the PDF values to momentum, calculation of the required PDF values to fix the velocity at a lattice node results in this single equation with 9 unknowns. This problem however can be avoided through the use of what is known as the bounce back boundary condition.[7]

In an LBM model a solid surface may be represented by a bounce back node, or series a of bounce back nodes. When a lattice node is deemed bounce back then any momentum incoming to the lattice node is reflected back towards the lattice node it came from in the subsequent time step, with no collision process occurring on the bounce back lattice node. This operation ultimately modifies the evolution equation for the lattice node in question to read as equation (12).

$$f_i(\mathbf{x} + \mathbf{e}_i \Delta t, t + \Delta t) = f_{-i}(\mathbf{x}, t) \tag{12}$$

where f_{-i} is the PDF who's associated vector points in the opposite direction to the PDF f_i.

Due to the simplicity of the bounce back boundary condition, its use is convenient but not ideal. He *et al.* showed that use of the bounce back boundary condition in an LBM model will degrade the accuracy of the model to first order in space.[7]

3.3 No Slip - Partial Bounce Back

The Partial Bounce Back (PBB) boundary condition refers to a specific use of the Immersed Moving Boundary (IMB) condition proposed by Noble & Torczynski.[4] The IMB condition is one which attempts to incorporate the interaction between a fluid and a solid body moving through it. An IMB may represent a boundary that does not conform to the computational grid, or lattice in this case, and this boundary may be moving with some velocity relative to the surrounding fluid. It can be seen in Fig. 2 that an object which does not conform to the computational lattice may only partially occupy any given lattice node; this may well be the case when considering a non-integer voxel taken from a micro-CT scan of a rock medium representing a definite fluid solid boundary intersecting the voxel. The IMB technique proposed by Noble & Torczynski results in a modification to equation (4) to read as:

$$f_i(\mathbf{x}+\mathbf{e}_i\Delta_t, t+\Delta_t) - f_i(\mathbf{x},t) = [1-B(\mathbf{x},\epsilon_s)]\,\Omega_i^{BGK} + B(\mathbf{x},\epsilon_s)\Omega_i^S \tag{13}$$

where,

$$\Omega_i^{BGK} = \frac{1}{\tau}(f_i^{eq}(\rho,\mathbf{u}_f) - f_i(\mathbf{x},t)) \tag{14}$$

and,

$$\Omega_i^S = f_{-i}(\mathbf{x},t) - f_i(\mathbf{x},t) + f_i^{eq}(\rho,\mathbf{u}_s) - f_{-i}^{eq}(\rho,\mathbf{u}_f) \tag{15}$$

or,

$$\Omega_i^S = f_{-i}(\mathbf{x},t) - f_i(\mathbf{x},t) + f_i^{eq}(\rho,\mathbf{u}_s) - f_{-i}^{eq}(\rho,\mathbf{u}_s) \tag{16}$$

in which $f_{-i}^{eq}(\rho,\mathbf{u}_s)$ and $f_{-i}^{eq}(\rho,\mathbf{u}_f)$ are the equilibrium particle distribution functions as given by equation (5) with $\mathbf{u}=\mathbf{u}_s$ and $\mathbf{u}=\mathbf{u}_f$ respectively. $\mathbf{u}_s$ is the velocity of the boundary, and $\mathbf{u}_f$ is the velocity of the fluid.

Equation (15) is the expression originally proposed for Ω_i^S; though another expression, equation (16), was proposed by Holdych[8] which has been shown to increase the accuracy of computed force and torque on a sphere in poiseuille flow when compared with the original expression.[9] In the interests of completeness both expressions were explored in this study with respect to the accuracy of measured permeability.

In equation (13), $B(\mathbf{x},\epsilon_s)$ is a function which represents a *solid fraction* field across the domain allowing for a different solid fraction, ϵ_s, at individual lattice nodes. In the the original paper Noble & Torczynski propose two formulations for $B(\mathbf{x},\epsilon_s)$; the first is direct use of solid fraction so that

$$B(\mathbf{x},\epsilon_s) = \epsilon_s(\mathbf{x}) \tag{17}$$

The second formulation is a function of ϵ_s with *relaxation time dependent weighting*

$$B(\mathbf{x}) = \frac{\epsilon_s(\mathbf{x})(\tau-1/2)}{(1+\epsilon_s(\mathbf{x}))+(\tau-1/2)} \tag{18}$$

which is reported to work well for τ between 0.6 and 0.9. Though the impact of the relaxation time dependent weighting is negligible, and was shown not to impact upon results.[10] Therefore the simpler form of $B(\mathbf{x},\epsilon_s)$ given by equation (17) was used in this study.

The effect of this modification to the Lattice Boltzmann Equation is essentially the partial application of the bounce back boundary condition to every lattice node. The strength of this partial application is dependent upon the velocity of the boundary, and the proportion of a lattice node which is occupied by the boundary, or porosity. This form of the PBB condition has previously been used by Feng *et al.* who have shown it

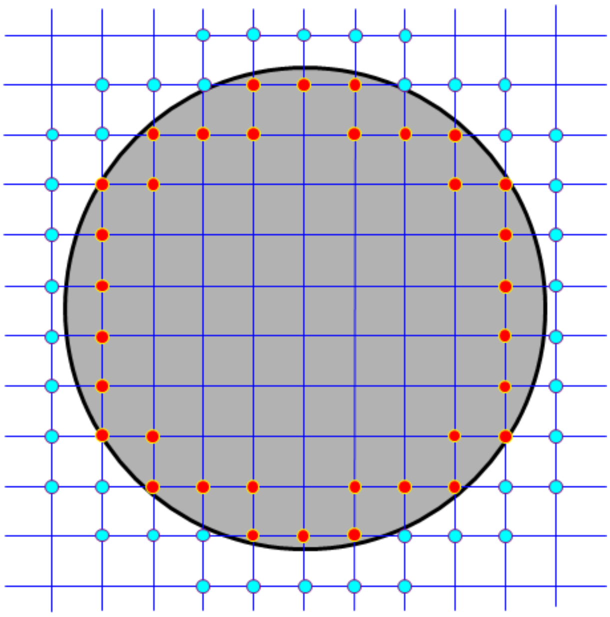

Figure 2: An example of a boundary which does not conform to the computational grid

to be a suitable choice for considering the interaction between the flow of a fluid and immersed objects in both 2D[10] and 3D.[11] Using such a boundary condition with the boundary velocity set to zero leaves us with the partial application of the bounce back condition scaling only with porosity. In this way, the proposed boundary scheme may be used to consider intrinsically porous lattice nodes. The relationship between resultant permeability and imposed porosity using the PBB condition with a zero boundary velocity was explored and results are presented in section 4.1.

The PBB condition allows for direct consideration of non-integer micro-CT voxels. Where a non-integer voxel would represent either a definite fluid/solid boundary or an intrinsically porous region of the medium, the ability of the PBB condition to consider such regions was explored in two tests models designed to represent each case.

3.4 Applied Pressure Drop

In order to use Darcy's equation to numerically approximate material permeability, a pressure gradient must be applied across the considered computational domain. To do this in the LBM model, the popular Zhou/He boundary condition has been used.[5] As has been stated, imposition of a specific value of density, pressure or momentum on any one lattice node is non-trivial. This is due to the fact that for the LBM there exists only one equation linking the desired macroscopic value to the microscopic PDF's, and since there are nine PDF's for a D2Q9 lattice we are left with one equation and 9 unknowns. In an attempt to circumvent this situation Zhou & He suggested two assumptions:

- A PDF who's origin is from within the computational domain is of the correct value
- A PDF who's origin is outside the boundary may be computed if the relationship proposed in equation (19) is respected for the PDF normal to the boundary (in this case f_1 is normal to the boundary)

$$f_1 - f_1^{eq} = f_3 - f_3^{eq} \tag{19}$$

If the stated assumptions are respected then one can apply some algebra to the LBM equations to gain expressions for the remaining non-normal PDF's which are streamed from outside the boundary. For straight boundaries Zhou & He demonstrate second order accuracy with their boundary technique on a D2Q9 lattice. The Zhou/He boundary condition can be used to specify pressure at both the inlet and the outlet of the computational domain. With differing inlet and outlet pressure imposed, a pressure gradient across the domain will establish itself as steady state is achieved.

4 RESULTS

To test the validity of using the PBB condition to model flows which include geometry that is either porous or partially occupying lattice nodes, such as may be gained from a micro-CT scan, two test cases were explored. These test cases were flow through a periodic array of hexagonally packed cylinders, demonstrating the methods ability to deal with lattice nodes partially occupied by a solid body; and flow through a simple heterogeneous porous media, demonstrating the methods ability to deal with porous bodies. The relationship between the porosity of a lattice node and its permeability was also explored. A description of the tests and commentary on results is included in this section.

4.1 Relationship Between Porosity and Permeability using the PBB condition

The PBB condition was used in this study to impose an intrinsic porosity upon individual lattice nodes within a computational domain. This novel use of the technique proposed by Noble & Torczynski requires first that the relationship between the porosity and permeability of a lattice node be defined. Since no equation was available to relate these factors an experiment was carried out. The experimental set up uses the PBB condition to consider a domain of uniform porosity, Zhou/He pressure boundaries were used to impose a pressure drop between the inlet and outlet of the domain, and the resultant flow rate was measured. From this a specific value of permeability can be calculated using Darcy's equation (1) to match a specific value of porosity. Different value's of porosity were tested from 0.05 to 0.95 in increments of 0.05. A plot of porosity versus permeability is included in Fig. 3 which shows an exponential relationship between porosity and permeability. In the interest of simplicity all tests were carried out with $\tau = 1$ and a fixed arbitrary pressure drop of 0.0005, the domain consisted of 100 lattice nodes in x and y.

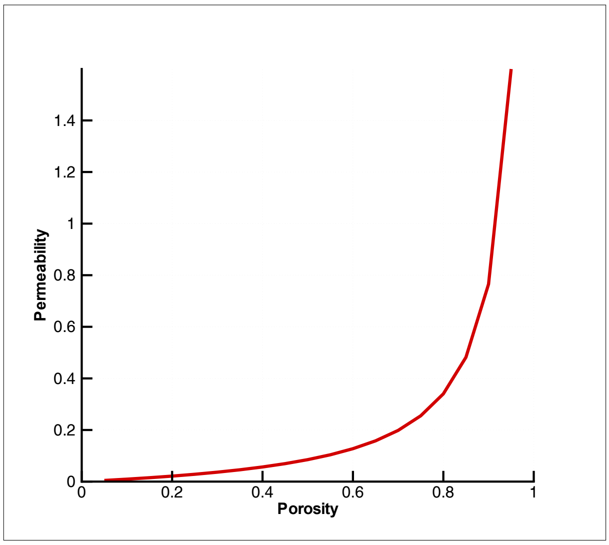

Figure 3: Relationship of Nodal Porosity and Nodal Permeability

4.2 Unit Cell Cylinder

The Unit Cell cylinder test is designed to test the accuracy of the PBB condition with respect to permeability of a domain where the PBB condition is used to consider nodes which are intersected by a definite fluid/solid boundary. The unit cell model is representative of a periodic array of hexagonally packed cylinders and a diagram of the unit cell geometry is included in Fig. 4.

To represent the cylinder geometry using the traditional bounce back technique would leave the cylinder under defined in a 'staircase' approximation, where the curve of the cylinder edge is staggered as it passes through individual lattice nodes. Those lattice nodes whose centre is within the cylinder radius are deemed bounceback, whereas those lattice nodes whose centre is outside of the cylinder radius are simply fluid lattice nodes. This leaves the cylinder under defined as under this approximation to the cylinder surface there would be lattice nodes which are partially intersected by the cylinder surface where the centre of the lattice node in question lies outside the cylinder radius. Such lattice nodes may be accounted for by using the PBB boundary condition taking into consideration the fraction of these lattice nodes which is occupied by the cylinder.

The permeability of a periodic array of hexagonally packed cylinders was independently studied by both Gebart[12] and Lee & Yang[13] who have proposed expressions for permeability normalised against the cylinder diameter. Equation (20) is the expression proposed by Gebart, while equation (21) is the expression proposed by Lee & Yang.

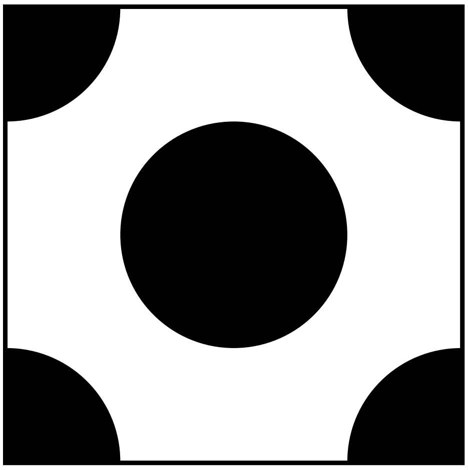

Figure 4: Geometry of Unit Cell Cylinder

$$\frac{k}{d^2} = \frac{4}{9\pi\sqrt{6}}\left(\sqrt{\frac{\pi/2\sqrt{3}}{1-\phi}}-1\right)^{5/2} \tag{20}$$

$$\frac{k}{d^2} = \frac{\phi^3(\phi-0.2146)}{31(1-\phi)^{1.3}} \tag{21}$$

For the unit cell cylinder test the expressions proposed by Gebart and Lee & Yang are used as a benchmark against which to compare numerical results. The LBM was tested with three alternate boundary conditions to represent the cylinder geometry, bounce back, PBB with Noble & Torczynski's original expression for Ω^s, and PBB with Holdych's expression for Ω^s. As with the experiment investigating the relationship between lattice node porosity and permeability, the Zhou/He pressure boundary was used at the inlet and outlet to impose a pressure drop of 0.0005 across the domain with $\tau = 1$. Numerical results were gained for two independent cases. The first test case was a series of models at a fixed resolution of 100 lattice nodes in x and y, with varying cylinder radius. This test was designed to evaluate the accuracy of the LBM using these boundary conditions across the range of possible porosities for the model. The second test case included a series of models with a fixed cylinder radius but varying resolution, that is the ratio between radius and resolution in lattice units was fixed; designed to evaluate the sensitivity of this technique to resolution. For the test case considering varying resolution the radius was fixed such as to give porosity of the model ≈ 0.65. For all test models a pressure drop is imposed, the resultant flux is measured, and the permeability is calculated using Darcy's equation (1).

Fig. 5 shows the results of the unit cell cylinder test for varying cylinder radius. The plot of diameter normalised permeability versus porosity shows that in the low ranges of

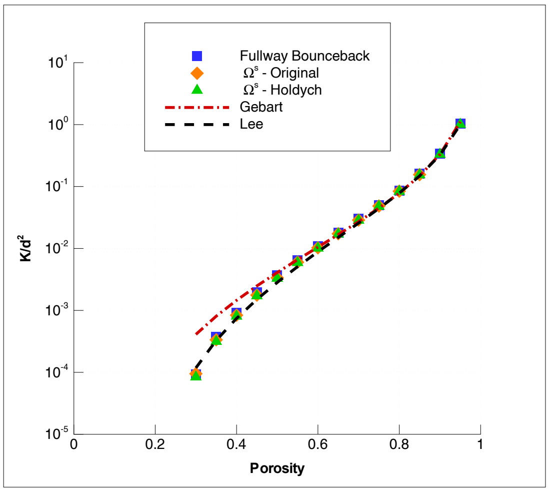

(a) Variation of K/d^2 with Porosity

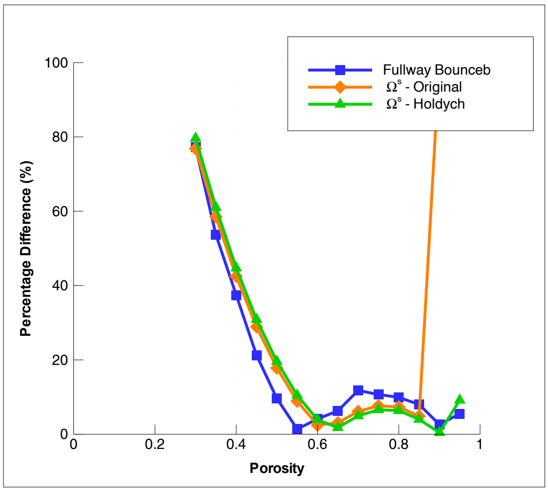

(b) Difference between numerical results and Gebart's Expression

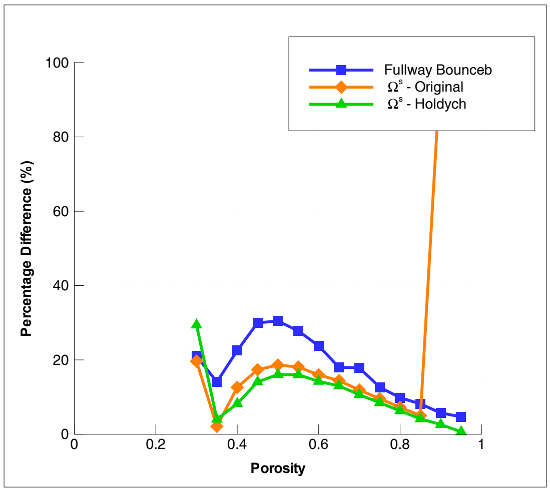

(c) Difference between numerical results and Lee & Yang's Expression

Figure 5: Results for Unit Cell Cylinder Model with Variation of Porosity

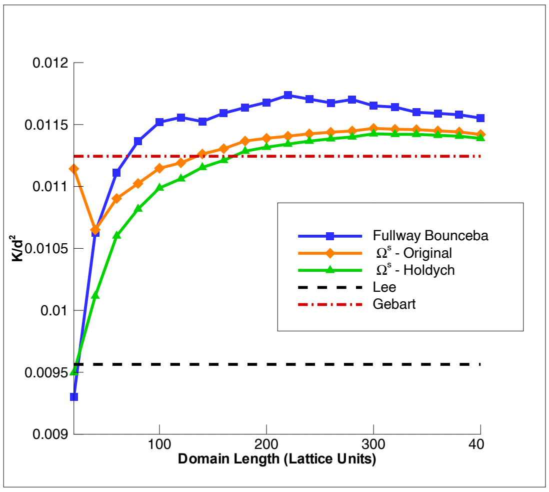

Figure 6: Results for Unit Cell Cylinder Model with Variation of Resolution

porosity, the results match closely to the expression proposed by Lee & Yang, as porosity increases, the results begin to agree more closely with Gebart's expression. Overall good correlation has been achieved between the numerical results and published expressions. The plots of percentage difference show that in general the results from the models using the PBB boundary condition agree more closely with the published expressions than the results gained from models using the traditional bounce back technique. Inspection of Fig. 5a also shows that although the variation of difference between the numerical results and the published expressions in figures 5b and 5c is in many cases large ($> 10\%$), the numerical results agree more closely with the published expressions than the expressions agree with themselves.

One point of interest from these results is that when using the PBB condition with Noble & Torczynski's original expression for Ω^s the models exhibit some odd behaviour. For the most part, models were terminated when the root mean square of the sum of the change in velocity between time steps is sufficiently small, too ensure good results the threshold for this value was set to 10^{-10}. However at high porosity, using Noble & Torczynski's original expression for Ω^s the root mean square of the sum of the change in velocity between time steps never fell below the threshold value.

Fig. 6 shows the results of the unit cell cylinder test for varying resolution. The plot demonstrates that up to a domain length of 200 lattice nodes in x and y, results can vary by a relatively large degree, after this point the dependence of results on domain resolution starts to become marginal as they begin to converge.

4.3 Simple Heterogeneous Porous Media

The simple heterogeneous porous media test is designed to evaluate how accurately the PBB condition is able to consider a medium which is completely and non-uniformly

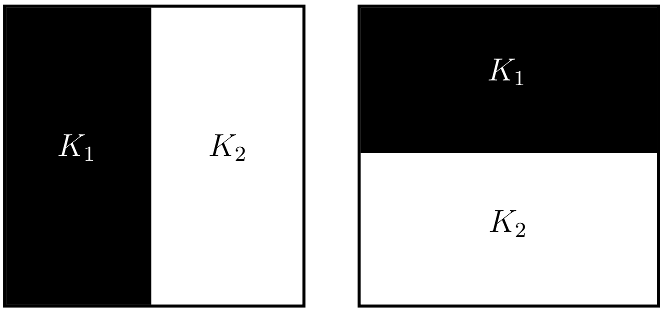

(a) Series (b) Parallel

Figure 7: Geometry of Heterogeneous Porous Media

porous. The test represents a simplified version of the case where a non-integer voxel from a micro-CT scan is the result of an area with intrinsic porosity, as opposed to a definite fluid/solid boundary. The computational domain to be considered is one which contains two regions of differing porosity, and thus permeability. Two such computational domains were used, one where these regions were aligned in parallel in the direction of flow, and one where these regions were aligned in series in the direction of flow. A diagram of this set up is included in Fig. 7.

Analytical expressions exist by which the effective permeability can be calculated if the permeability of the individual regions is known.[14] Analytical expressions for effective permeability of such simple media can be derived for both the medium in series and in parallel. If h_j is the width or height of a permeability region, and k_j is the corresponding permeability of this region, then the effective permeability of the region may be found as,

$$\text{Series:} \quad k_{eff} = \frac{\sum_{j=1}^{n} h_j}{\sum_{j=1}^{n} \frac{h_j}{k_j}} \tag{22}$$

$$\text{Parallel:} \quad k_{eff} = \frac{\sum_{j=1}^{n} h_j k_j}{\sum_{j=1}^{n} h_j} \tag{23}$$

For this test the models were set up so that a pressure drop is applied between the inlet and outlet the domain using the Zhou/He pressure boundary condition as with the other test cases. The resultant flowrate is measured and the permeability is again calculated using Darcy's equation (1). The models in series and in parallel were tested against increasing permeability difference between the two regions, where the maximum permeability difference is the case when region one has a porosity of 0.05 and region two has a porosity of 0.95. The results of this test are shown in figures 8 and 9 for the medium in series and in parallel respectively.

The results for the heterogeneous porous medium in series show excellent agreement

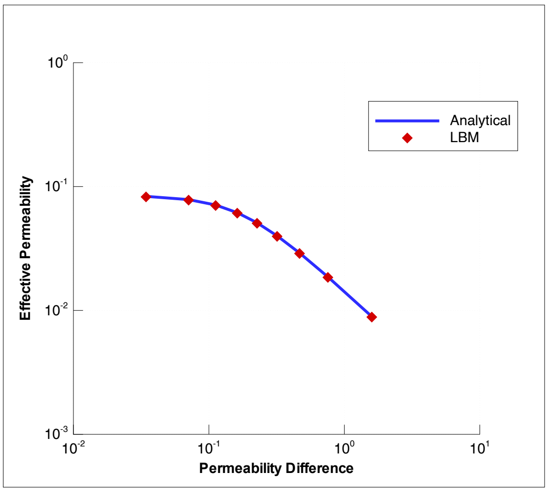

(a) Variation of Effective Permeability with Permeability Difference

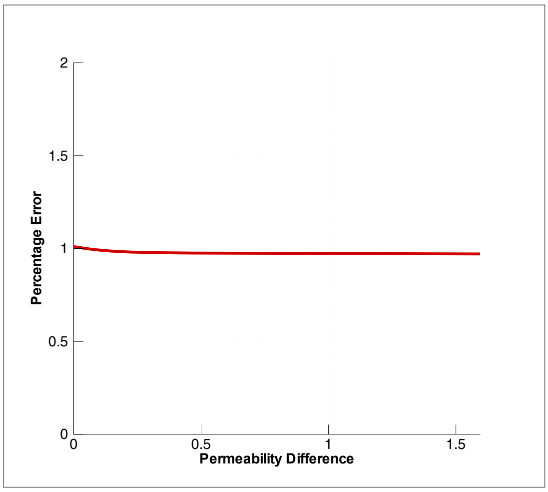

(b) Variation of Percentage Error with Permeability Difference

Figure 8: Results for Simple Heterogeneous Porous Media Model Aligned in Series

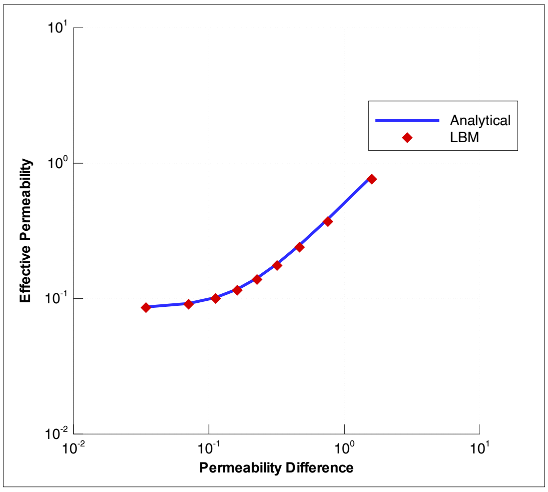

(a) Variation of Effective Permeability with Permeability Difference

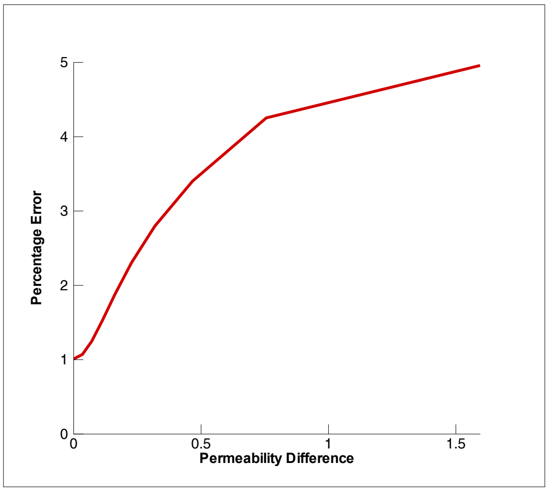

(b) Variation of Percentage Error with Permeability Difference

Figure 9: Results for Simple Heterogeneous Porous Media Model Aligned in Parallel

between the numerical and analytical effective permeability, with an almost constant error of $\approx 1\%$. The results for the heterogeneous porous medium in parallel are almost as good as for the medium in series, where the error for the smallest permeability difference being $\approx 1\%$ and the error for the largest permeability difference being $\approx 5\%$.

5 CONCLUSION

The goal of this study was to test the PBB boundary condition and assess its ability to deal with the type of geometry that would be gained from a micro-CT scan of porous rock. To this end the relationship between lattice node porosity and permeability was explored and reported. The PBB condition was then used to evaluate two test cases; flow past a periodic array of cylinders, and simple heterogeneous porous media. It was found that the PBB boundary condition is capable of considering boundaries which do not conform to the computational grid more accurately than if the standard bounce back boundary condition is used to represent these boundaries. In addition to this it was also shown in this test that Holdych's expression for Ω^s is indeed more accurate than Noble & Torczynski's original expression. It has also been shown that the PBB boundary condition is able to accurately predict the effective permeability of simple heterogeneous porous media with a maximum error of 5%. These facts lead us to the conclusion that the PBB boundary condition is a suitable choice for modelling the flow through a voxelised representation of the internal micro structure of a rock, while maintaining the definition of the geometry as determined by a micro-CT scan. Further work will explore the presented test cases in 3D, and ultimately lead to computational analysis of real rock geometries.

REFERENCES

[1] Xiaoyi He and Li S. Luo. Theory of the lattice boltzmann method: From the boltzmann equation to the lattice boltzmann equation. *Physical Review E*, 56(6):6811–6817, December 1997.

[2] Aydin Nabovati, Edward W. Llewellin, and Antonio C.M. Sousa. A general model for the permeability of fibrous porous media based on fluid flow simulations using the lattice boltzmann method. *Composites Part A: Applied Science and Manufacturing*, 40(6-7):860 – 869, 2009.

[3] Edo S. Boek and Maddalena Venturoli. Lattice-boltzmann studies of fluid flow in porous media with realistic rock geometries. *Computers & Mathematics with Applications*, 59(7):2305 – 2314, 2010.

[4] D.R. Noble and J.R. Torczynski. A lattice-boltzmann method for partially saturated computational cells. *International Journal of Modern Physics C*, 9:1189–1201, 1998.

[5] Qisu Zou and Xiaoyi He. On pressure and velocity boundary conditions for the lattice boltzmann bgk model. *Physics of Fluids*, 9(6):1591–1598, 1997.

[6] P. L. Bhatnagar, E. P. Gross, and M. Krook. A model for collision processes in gases. i. small amplitude processes in charged and neutral one-component systems. *Phys. Rev.*, 94(3):511–525, May 1954.

[7] Xiaoyi He, Qisu Zou, Li-Shi Luo, and Micah Dembo. Analytic solutions of simple flows and analysis of nonslip boundary conditions for the lattice boltzmann bgk model. *Journal of Statistical Physics*, 87:115–136, 1997.

[8] D. J. Holdych. *Lattice Boltzmann methods for diffuse and mobile interfaces*. PhD thesis, University of Illinois at Urbana-Champaign, 2003.

[9] O. Erik Strack and Benjamin K. Cook. Three-dimensional immersed boundary conditions for moving solids in the lattice-boltzmann method. *International Journal for Numerical Methods in Fluids*, 55(2):103–125, 2007.

[10] Y. T. Feng, K. Han, and D. R. J. Owen. Coupled lattice boltzmann method and discrete element modelling of particle transport in turbulent fluid flows: Computational issues. *International Journal for Numerical Methods in Engineering*, 72(9):1111–1134, 2007.

[11] Y. T. Feng, K. Han, and D. R. J. Owen. Combined three-dimensional lattice boltzmann method and discrete element method for modelling fluidparticle interactions with experimental assessment. *International Journal for Numerical Methods in Engineering*, 81(2):229–245, 2010.

[12] B.R. Gebart. Permeability of unidirectional reinforcements for rtm. *Journal of Composite Materials*, 26(8):1100–1133, 1992.

[13] S. L. Lee and J. H. Yang. Modeling of darcy-forchheimer drag for fluid flow across a bank of circular cylinders. *International Journal of Heat and Mass Transfer*, 40(13):3149 – 3155, 1997.

[14] Y. Gao and M. M. Sharma. A lga model for fluid flow in heterogeneous porous media. *Transport in Porous Media*, 17:1–17, 1994.